Combined dynamic programming and region-elimination technique algorithm for optimal sizing and management of lithium-ion batteries for photovoltaic plants

Alberto Berrueta[a], Michael Heck[b], Martin Jantsch[b], Alfredo Ursúa[a], Pablo Sanchis[a,*]

[a] *Department of Electrical and Electronic Engineering, Institute of Smart Cities, Public University of Navarre, Campus de Arrosadia, 31006 Pamplona, Spain*
[b] *Fraunhofer Institute for Solar Energy Systems ISE, Heidenhofstraße 2, 79110 Freiburg, Germany*

Abstract

The unpredictable nature of renewable energies is drawing attention to lithium-ion batteries. In order to make full utilization of these batteries, some research works are focused on the management of existing systems, while others propose sizing techniques based on business models. However, in order to optimise the global system, a comprehensive methodology that considers both battery sizing and management at the same time is needed. This paper proposes a new optimisation algorithm based on a combination of dynamic programming and a region-elimination technique that makes it possible to address both problems at the same time. This is of great interest, since the optimal size of the storage system depends on the management strategy and, in turn, the design of this strategy needs to take account of the battery size. The method is applied to a real installation consisting of a 100 kWp rooftop photovoltaic plant and a Li-ion battery system connected to a grid with variable electricity price. Results show that, unlike conventional optimisation methods, the proposed algorithm reaches an optimised energy dispatch plan that leads to a higher net present value. Finally, the tool is used to provide a sensitivity analysis that identifies key informative variables for decision makers.

Keywords: Energy storage system, Lithium-ion battery, Optimal energy dispatch scheduling, Dynamic programming method, Energy arbitrage, Renewable energy

Nomenclature

Variables

α	Calendar ageing coefficient	–
β	Cycle ageing coefficient	–
a	fitting parameter	–
b	Fitting coefficient	–
C	Capacity	Ah
$Cost$	Economic cost	EUR
g	Inflation	p.u.
GHI	Global horizontal irradiance	$\mathrm{W\,m^{-2}}$
i	Current	A
IR	Interest rate	p.u.
J	Objective function	EUR
k	Counter	–
$Life$	Lifetime	years
N	Number of time steps	–
n	Integer number	–
NPV	Net present value	EUR
P	Power	W
PC	Price	EUR
Q	Electric charge	Ah
R	Resistance	Ω
Rev	Annual profit	EUR
SOC	State of charge	p.u.
SOH	State of health	p.u.
t	Time	h or years
v	Voltage	V

Subscripts

$_0$	Independent or initial
$_1$	Linear term
$_2$	Quadratic term
$_{bat}$	Battery
$_{cell}$	Battery cell
$_{cyc}$	Cycle
$_C$	Capacity
$_{DC}$	Direct current
$_{DOD}$	Depth of discharge
$_{elec}$	Electricity
$_{exp}$	Exponential
$_{grid}$	Electricity grid

*Corresponding author

inv	Inverter
I	Current
i	Internal
j	Either among various options
$loss$	Losses
max	Maximum value
min	Minimum value
N	Nominal value
$O\&M$	Operation and maintenance
OC	Open circuit
pan	PV pannel
$peak$	Peak value
PV	Photovoltaic
R	Resistance
T	Temperature
v	Voltage

Superscripts

*	Maximum available

1. Introduction

The energy sources used to produce electricity are experiencing a rapid change from traditional fossil fuels to renewable energies [1]. A distinctive feature of renewable energy is its unpredictability, which can cause a number of problems to the electricity grid, such as network overloading during periods with high renewable generation [2, 3], being one of the major concerns highlighted by consultants and specialists. Network areas with high photovoltaic (PV) production need to manage a high power flow during periods of high irradiance, yet they are underused during the rest of the day. Power curtailment has been studied as a solution to this problem in the European Research project Insight_E [4], however its main disadvantage is that a significant proportion of the renewable energy available is discarded as a result of this curtailment. In order to reduce the amount of discarded energy, other energy services, such as energy arbitrage, peak shaving and demand side management, can be implemented as alternative options to curtailment. All these services require the use of an energy storage system (ESS). The rapid reduction in the price of Li-ion batteries is focussing interest on these alternatives.

A cost benefit analysis of PV–battery plants published in 2013 [5] concluded that the addition of a battery to a PV system would be profitable if the battery cost were between USD 400 and USD 500 per kWh (EUR 326 to EUR 407 per kWh), something which is now a reality. In fact, the price of the Tesla Powerwall 2 (14 kWh) small-scale, stationary battery with integrated power converter is already USD 490 per kWh excluding taxes (EUR 400 per kWh) [6]. Prices for large-scale battery systems are monitored by institutions such as the U.S. Department Of Energy (DOE) which reported a drop from around USD 1,000 per kWh in 2008 (EUR 815 per kWh) to USD 268 per kWh in 2015 (EUR 218 per kWh). It also set a target of USD 125 per kWh by 2022 (EUR 102 per kWh), as summarised by the IEA in a report published in 2016 [7]. Even though the current reduction in the battery price is significant, considerable investment is still required for the installation of an ESS in a renewable-energy plant. Therefore, its optimal sizing and management need to be studied in order to achieve a competitive power plant.

Two approaches are usually proposed to design ESSs with renewable systems. Firstly, the economic approach focuses on the profitability of the investment required to set up an ESS. The target of these studies is to analyse the economica feasibility of an ESS in a a particular environment [8]. In this respect, the levelised cost of energy (LCOE) of a PV system is studied in [9], where the authors propose a variable termed levelised cost of dispatch (LCOD), which is slightly different from the LCOE. Other authors analyse the role of the incentives applied to renewable energies [10] or the influence of the electricity tariff on the profitability of the system [11]. Moreover, Lombardi and Schwabe propose a business model based on shared economy to increase the profitability of an ESS. Finally, other authors particularise the case studied for either a domestic [12] or commercial photovoltaic system [13]. All these studies are primarily focused on economic aspects. However, given the fact that their aim is not the management of the ESS, the battery operation is significantly simplified. Many of these works model the electrical performance of the battery by constant efficiency, and the ageing behaviour is either not considered or is included by a simple charge–discharge cycle counting method. This is particularly problematic, since ageing behaviour is of high importance for the profitability of the ESS, as highlighted by a number of research works on the use of batteries for the grid integration of renewable-energy plants such as microgrids [14], wind power plants [15] and photovoltaic plants [16]. Due to all these simplifications, the system performance cannot be taken into account, being these studies not suitable for either online battery management or optimal battery sizing.

The second approach to the design of renewable-based ESS focusses on battery management. Some authors centre their attention on the effect that the battery has on the electricity grid [16] and propose different grid services to be provided by an ESS [17], analysing variables such as PV self-sufficiency [18] or the self-consumption of domestic PV systems [19]. Other authors propose different

optimisation methods for the management of ESSs where, yet again, no particular attention is paid to battery ageing, even though the consideration of these phenomena has been proven to enhance the functionality of a battery [20]. One of the most common methods is linear programming, which is used to design the battery charging strategy [21] or the management of grid-connected [5] and residential [22] PV–battery systems. Linear optimisation is computationally efficient, but the models involved need to be linearised, which can be a source of inaccuracy in the results [23]. A number of non-linear algorithms have been proposed when higher accuracy is required [24]. Some research works propose neural networks [25] and non-linear optimisation techniques [26] to optimise the battery energy dispatch. However these authors are not particularly concerned with optimising the battery size or with ageing considerations. The algorithms mentioned only deal with the battery management.

It can therefore be seen that there is a lack of comprehensive algorithms able to make a complete analysis of a PV–battery system by taking into account relevant factors such as non-linear battery ageing, technical constraints and economical variables. In this paper, we propose an integrated approach to this problem, addressing both the battery sizing and management at the same time. This approach is of great interest, since the optimal size of an ESS depends on its power requirements determined by the management strategy, while optimal battery management depends on its size. With this aim, we propose a novel optimisation algorithm based on a combination of dynamic programming and a region-elimination technique. This algorithm can deal with non-linear models of both the battery electrical performance and its ageing behaviour, thus improving the accuracy and reliability of the results. It is a flexible algorithm that can easily be used with different system models. In order to show its applicability, specific advanced, non-linear models are introduced and used in this paper. The algorithm is headed towards its direct applicability, considering the case study of a rooftop grid-connected industrial PV system where real-life measurements of irradiance and electricity prices are included. As shown in this paper, the improvement achieved by the proposed global optimisation is quantified as 22% compared to the sequential consideration of battery size and management. Finally, the main concepts studied by the above-mentioned economic analyses are compiled in a sensitivity analysis of the case study.

The approach presented in this paper offers three main differences compared to other published works: (i) the optimisation algorithm, based on the combination of dynamic programming with a region-elimination technique, addresses the overall optimisation of sizing and management of the ESS taking system nonlinearities into account, which assures a global optimal solution for the PV–battery system, (ii) it is applied to a real rooftop industrial PV system, in contrast to the typical domestic and microgrid applications, an scenario that is gaining importance due to the increasing installation of PV power in industrial estates, and (iii) the sensitivity analysis presented in the final part of the paper as an application of the proposed methodology provides results that are particularly useful to a number of decision makers.

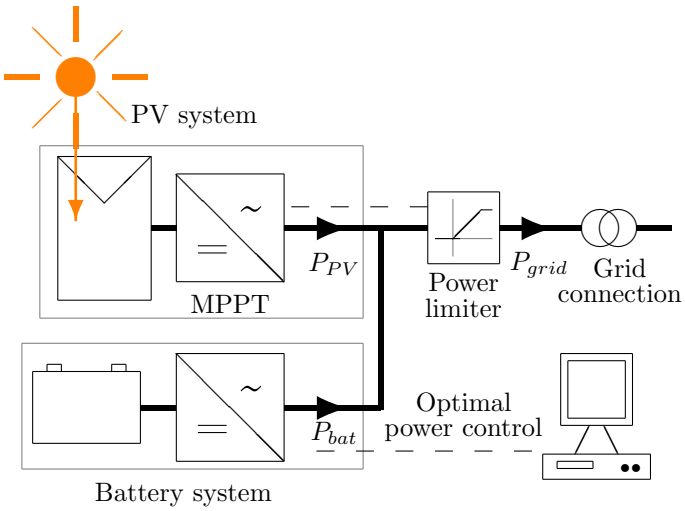

Figure 1: System diagram of the PV+ plant.

This paper is organized into six sections. Firstly, in Section 2, the case study used to particularise the proposed optimisation algorithm, along with the models of each system is explained. Then, Section 3 gives an insight into the mathematical equations required for the programming of the optimisation algorithm. Subsequently, the optimisation algorithm is compared in Section 4 with other battery management algorithms proposed in the literature showing the most noteworthy results in a comparative table. Section 5 then presents an application of this optimisation method, which is a sensitivity analysis that quantifies the influence of different parameters in battery profitability. Finally, Section 6 summarizes the conclusions of the paper.

2. Case study

2.1. General description of the case study

The optimisation method proposed in this paper is applied to a medium-sized PV plant with a peak power of 100 kW connected to the 13.2 kV distribution network of an industrial estate located in Navarra, in the north of Spain. As shown in Figure 1, the PV system comprises the PV array and the PV inverter. The PV array is formed

by the connection of $n_{pan} = 470$ PV panels made by the company Yingli Solar (YL250P–29b, with a peak power of $P_{pan} = 250$ Wp). The peak power of the PV array is the DC power generated with optimal solar radiation and standard ambient temperature, which is only achieved for a few hours throughout the year:

$$P_{peak} = n_{pan} \cdot P_{pan} = 117.5 \text{ kWp} \quad (1)$$

A common design strategy is to oversize the output power of the PV array in relation to the PV inverter, so that it is not possible to generate the whole P_{peak} during the few hours with maximum irradiance. As an advantage, the price of the inverter is lower and it has enhanced efficiency at the more common lower irradiance levels. An accepted sizing rule is for the nominal power of the PV inverter to be set to $P_{PV,inv} = 0.85 \cdot P_{peak} \approx 100$ kW [27]. The power converter used is the IS 3PLAY, made by the company Ingeteam, with a rated power of 100 kW. The control algorithm of the PV inverter is the maximum power point tracker (MPPT) designed to maximize the power generated by the PV modules. The maximum power that could be generated by the PV array is denoted as P^*_{PV}. In a normal situation, the MPPT achieves this PV power, and $P_{PV} = P^*_{PV}$. However, as the saturation of the distribution network is a concern in industrial estates, a feed-in power limitation is considered. As an interesting limit proposed in various countries, the selected value is 60% of the inverter nominal power. Therefore, when a power higher than the maximum feed-in power ($P_{grid,max}$) is injected into the grid, the PV inverter power is limited, as shown in Figure 1 and the extra available power is not generated ($P_{PV} \leq P^*_{PV}$). P_{grid} is assumed to be unidirectional from the plant to the grid, since regulations in most countries do not permit the supply of grid power to the generation plant. Measured meteorological data during the year 2016 in Spain are taken from the free-access database Meteonavarra [28]. The data were recorded by a weather station named *Bardenas*, with an annual solar radiation of around 1,700 kWh m^{-2}. The mentioned technical characteristics of the case study are summarised in Table 1.

Table 1: Main technical specifications of the case study.

Characteristic	Value
PV panel	Yingli Solar YL250P–29b
PV peak power	117.5 kW
PV inverter	Ingeteam IS 3PLAY
PV inverter rated power	100 kW
Battery converter	FeCon BAT50
Battery converter power	50 kW
Feed in limitation	60% of the inverter power
Grid voltage	13.2 kV
Annual solar radiation	1,700 kWh m^{-2}

The battery storage system consists of a Li-ion battery pack and a bidirectional battery power converter used to connect it to the AC grid. The battery pack is built by the series and parallel connection of a number of Li-ion cells that needs to be determined in a trade-off between a low price and a long battery lifetime. Two services are provided by the battery in this scenario. On the one hand, the energy generated by the PV modules can be increased, since the shaved peaks are stored and delivered when the grid is not overloaded, which is a service to the utility grid manager. On the other hand, the stored electricity is sold when its price is at its highest, providing greater economic revenue to the PV plant owner. It is interesting to make the analysis under realistic, variable electricity prices. However, as mentioned above, some grid services are not properly remunerated, based on current market rules. Therefore, the real electricity price in Spain during 2016 is scaled up to an average price of EUR 0.14 per kWh maintaining the current variability of market prices. A price of EUR 250 per kWh for the battery system is considered, which includes the cost of the battery bidirectional power converter. This price is lower than the system cost in the current market, but can be a realistic approach for the near future. The optimisation method proposed in this paper aims to maximise the economic revenue of the PV system. Therefore the Net Present Value (NPV) is chosen as the figure of merit for comparability between different results, which is defined by Dufo López and Bernal-Agustín [29] as follows:

$$NPV = -Cost_{bat} + \sum_{k=1}^{Life} Rev \cdot \frac{(1+g_{elec})^k}{(1+IR)^k} - Cost_{O\&M} \frac{(1+g_{O\&M})^k}{(1+IR)^k} \quad (2)$$

where $Life$ is the battery lifetime expressed in years, Rev is the annual profit achieved by the inclusion of the battery system, $Cost_{bat}$ is the battery cost and $Cost_{O\&M}$= EUR 1 per kWh per year is the annual operation and maintenance costs, whose value is proposed by Dufo López and Bernal-Agustín [29]. The values of the remaining variables from Equation 2, which are economic magnitudes, are: g_{elec}=3% is the inflation for electricity prices, $g_{O\&M}$=2% inflation for O&M costs and IR=4% is the interest rate [29].

Given the importance of the model accuracy in obtaining representative results, robust and reliable models are used for the PV arrays, PV and battery inverters and Li-ion battery pack. The models used are detailed in the following subsections.

2.2. PV system modelling

The conversion of solar irradiance to electric power is modelled using the PVLIB toolbox, which is a set of open-source modelling functions for simulating the performance

Table 2: Value of the parameters for the power converters models.

		Parameter	Value	Unit
PV inverter		b_0	298	W
		b_1	$2.01 \cdot 10^{-3}$	–
		b_2	$1.64 \cdot 10^{-7}$	W^{-1}
Batt. converter	Charge	b_0	112	W
		b_1	$3.36 \cdot 10^{-3}$	–
		b_2	$2.22 \cdot 10^{-7}$	W^{-1}
	Disch.	b_0	137	W
		b_1	$3.28 \cdot 10^{-3}$	–
		b_2	$2.46 \cdot 10^{-7}$	W^{-1}

of photovoltaic energy systems provided by Sandia National Laboratories [30]. The inputs for this toolbox are the PV plant location, global horizontal irradiance, temperature, size of the PV array and orientation of the modules. To perform the simulation, PVLIB calculates the relative position of the sun and, using horizontal irradiance data and an atmosphere model, divides this global irradiance into its direct and diffuse components. With these variables, the ambient temperature, the module orientation and the array size, the PV cell temperature and I–V characteristics are calculated, and subsequently the output power.

The DC to AC conversion is modelled through the Driesse model [31], which takes into account power and input voltage in the calculation of inverter efficiency, as shown below:

$$P_{PV} = P_{PV,DC} - P_{PV,loss} \tag{3}$$

$$P_{PV,loss} = b_0 + b_1 \cdot P_{PV,DC} + b_2 \cdot P_{PV,DC}^2 \tag{4}$$

where $P_{PV,loss}$ are the power losses in the PV power converter (labelled as "MPPT" in Figure 1), and b_0, b_1 and b_2 are the empirical, voltage-dependent coefficients shown in Table 2. This approach takes into account self consumption, voltage drops and resistive losses. This inverter model was complemented by the panels characteristics provided by the databases included in PVLIB, which increase the reliability of the simulation results.

2.3. Battery system modelling

In order to model the battery system, models for the power converter and battery pack are required. The bidirectional battery converter is modelled using the equations described above for the PV inverter [32]. Based on the Driesse model, the performance of the battery converter is modelled through Equation 3 and Equation 4, using the parameters shown in Table 2, which take different values for either direction of the power flow.

The battery pack (see Figure 2 (a)) is modelled by the series and parallel connection of single Li-ion cells, each cell has an ageing behaviour that depends on the operating parameters. The battery model consists of an electric circuit representing the battery as a SOC-dependent voltage source and internal series resistance R_i.This equivalent circuit models the battery efficiency with high accuracy, given that it takes into account is current and SOC dependencies. The model reflects only static behaviour since the time steps for optimization are 1 h. The SOC defines the stored capacity relative to the actual full capacity ($C(SOH)$):

$$SOC(t) = SOC(t_0) - \int_{t_0}^{t} \frac{i_{bat}(t)}{C(SOH)} dt \tag{5}$$

The SOH is calculated with the ageing model, described below. Note that the negative sign before the integral term is due to the sign of the current i_{bat} defined as battery discharging current to be consistent with the sign of P_{bat}, i.e. discharging current if $i_{bat} > 0$.

In the battery storage system, Li-ion cells with NMC cathode and graphite anode are modelled. The dependence of open circuit voltage v_{OC} on SOC is determined by means of laboratory experiments proposed in the bibliography, such as low current charges and discharges [33, 34] and stepped-current charges and discharges [35], as shown in Figure 2 (b). This characteristic curve remains virtually constant for the whole battery lifetime [36] and is included in the model as a lookup table. The internal resistance R_i also depends on SOC, and has been determined with a current pulse method every 5%SOC, with the results shown in Figure 2 (c). As the battery ages, this parameter is scaled up, as detailed below.

The battery ageing model is a key tool for this optimisation algorithm, since the battery capacity decreases over its lifetime and depends on the calculated dispatch power. A common approach to battery ageing is a study of individual cells, given that they are easy to handle. Thanks to advanced SOH battery pack monitoring systems [37], it has been shown that the ageing performance of a pack does not significantly differ from that of a single cell. A recent study quantifies the discrepancy as 2%, and attributes it to temperature distribution [38]. Therefore, a cell model is used in this paper to predict the battery ageing. Battery ageing is divided into calendar and cycle ageing, which are normally assumed to be independent of each other and their effects are added together [39]. Based on the conclusion of a recent calendar ageing study [40], a linear time dependency of capacity fade and resistance rise is assumed, as shown in Equation 6 and Equation 7. For the cycle ageing modelling, the conclusions of three studies [41–43] are applied and the dependence of capacity fade and impedance rise with the number of equivalent

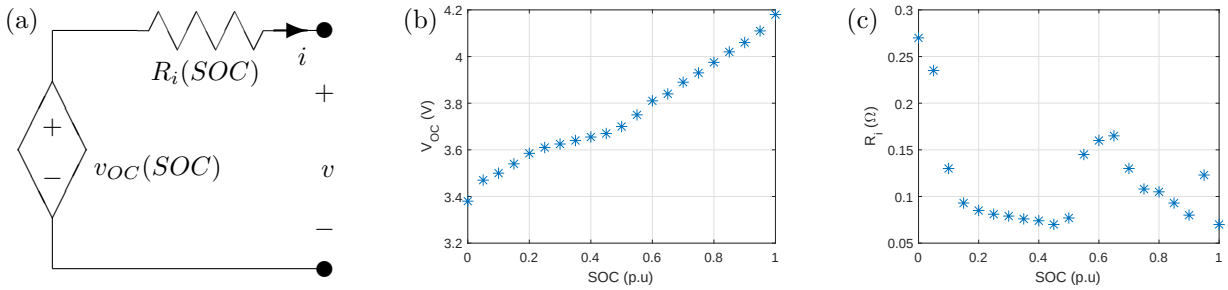

Figure 2: Cell electrical model: Equivalent circuit (a), v_{OC}–SOC relationship (b) and R_i–SOC relationship (c).

cycles Q is assumed to be also linear:

$$\frac{\Delta C(t,Q)}{C(t)} = -\left(\alpha_C \cdot t + \beta_C \cdot Q\right) \tag{6}$$

$$\frac{\Delta R_i(t,Q)}{R_i(t)} = \alpha_{R_i} \cdot t + \beta_{R_i} \cdot Q \tag{7}$$

where t is expressed in years and Q in equivalent full cycles. These expressions represent the capacity fade ($\Delta C = C(t) - C(t-\Delta t)$) and impedance rise ($\Delta R_i = R_i(t) - R_i(t-\Delta t)$) suffered by the battery during the analysed time lapse Δt.

Parameters α_j (j representing C and R_i) determine the calendar ageing, while β_j govern the cycle ageing. These four parameters are not constant, since calendar ageing is faster for increasing SOC and temperature [40] and cycle ageing is faster for higher current [41], average voltage and depth of discharge (DOD) [43]. These dependencies of α_j and β_j are modelled using the following expressions:

$$\alpha_j = a_{v,j} \cdot (v_{cell} - a_{0,j}) \cdot exp\left(-\frac{a_{T,j}}{T}\right) \tag{8}$$

$$\beta_i = b_{0,j} + b_{v,j} \cdot (v_{cyc} - b_{v0,j}).^2 + b_{DOD,j} \cdot DOD + b_{I,j} \cdot exp(b_{exp} \cdot \frac{|i_{bat}|}{C}) \tag{9}$$

With these expressions, calendar ageing has a linear dependency on the cell voltage and the temperature effect is modelled by an Arrhenius expression, as proposed in [43]. Given that Li-ion batteries require the operating temperature to be controlled, the battery temperature is assumed to be constant for this case study, being T=30°C in Equation 8. The cycle ageing has a quadratic dependence on average cycle voltage (v_{cyc}), a linear relationship with DOD [43] and an exponential trend with current, as modelled in [41]. These are the main variables reported to drive Li-ion battery calendar and cycle ageing, which are taken into account in this model through the parameters shown in Table 3.

It is noteworthy that the proposed ageing model is valid for what is termed the linear region of the battery lifetime,

Table 3: Battery ageing model parameters for ΔC (first column) and ΔR_i (second column) calculation.

	Parameter	Unit	ΔC	ΔR_i
Calend.	a_v	–	$2.716 \cdot 10^5$	$9.486 \cdot 10^3$
	a_0	V	3.1482	3.096
	a_T	K	6976	5986
Cycle	b_0	–	$2.71{\cdot}10^{-5}$	$2.28{\cdot}10^{-5}$
	b_v	V^{-1}	$3.14{\cdot}10^{-4}$	$3.208{\cdot}10^{-4}$
	b_{v0}	V	3.683	3.741
	b_{DOD}	–	$1.61{\cdot}10^{-6}$	$3.404{\cdot}10^{-6}$
	b_I	–	$1.56{\cdot}10^{-5}$	$1.56{\cdot}10^{-5}$
	b_{exp}	h	1.8	1.8

which occurs when capacity fade and impedance rise are below 20% of their nominal values [44]. After that, both ageing processes are accelerated and the battery lifetime is usually considered to be over. In this context, ΔSOH is defined as follows:

$$\Delta SOH = -\frac{1}{0.2} \cdot \max\left[\left|\frac{\Delta C}{C}\right|, \left|\frac{\Delta R_i}{R_i}\right|\right] \tag{10}$$

3. Optimisation algorithm

We propose in this section an optimisation algorithm aimed at the maximisation of the economic revenue obtained by the inclusion of a battery in a PV system such as the one described in Section 2. The optimisation problem consists in determining the battery size and power dispatch plan that maximize the value of an objective function. An optimisation method that combines dynamic programming with a region-elimination technique (as shown in Figure 3) is proposed to address this problem. It consists of an iterative algorithm with n iterations. Each iteration is an optimisation of the battery management during a complete year of system operation followed by the calculation of the value that the objective function has for this year. A region-elimination technique is then used to update the battery capacity. The proposed algorithm is explained in detail in the following subsections.

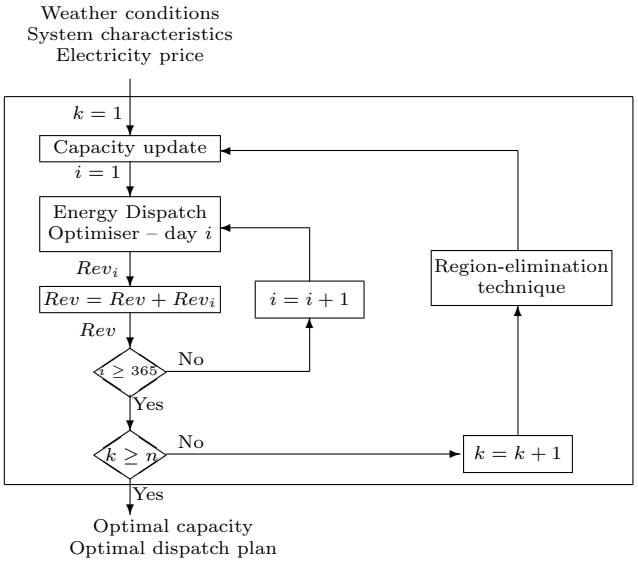

Figure 3: Flow diagram of the optimisation algorithm. The energy dispatch optimisation is run for a whole year, being Rev_i the revenue achieved during the day i and Rev the total revenue of the year. After this annual analysis, the battery capacity is updated by means of the region-elimination technique. This algorithms is repeated n times for the capacity size and energy management optimisation.

3.1. Objective function and constraints

The optimisation algorithm combines the models explained in Section 2 with an objective function and a number of operational constraints. The objective function J is an economic revenue obtained by the inclusion of a battery in the PV plant. This revenue comes, as explained in Section 2, from the combined effect of the augmented PV energy injected into the grid and the displacement of the PV generation to the time interval with highest energy price. The battery ageing costs are accounted by deducting, from the total profit of a time interval, the fraction of the battery cost corresponding to the capacity fade during that time. The proposed expression is shown in the following equation:

$$J = \int_{t_0}^{t} [(P_{grid,\text{PV–bat}} - P_{grid,\text{PV}}) \cdot PC_{elec} + \Delta SOH \cdot PC_{bat}]\, dt \quad (11)$$

where $P_{grid,\text{PV–bat}}$ is the power output of a PV–battery plant and $P_{grid,\text{PV}}$ is the power output of the PV plant with no battery. The economic variables involved in this expression are PC_{elec}, which is the price of electricity (in EUR per kWh), and PC_{bat}, which is the purchase price of the Li-ion battery (in EUR).

The constraints of the battery storage system , PV system, the feed-in power limitation and the battery converter

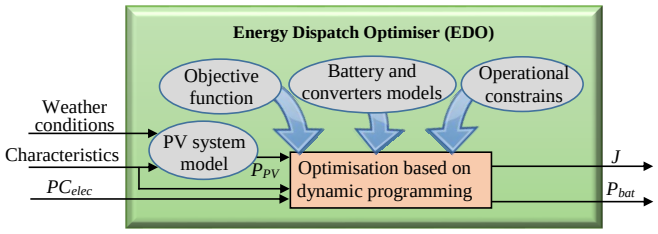

Figure 4: Schematic of the EDO. Input variables (weather conditions, electricity price and system characteristics), internal tools (objective function, operational constraints and models of the PV system, battery and power converters) and output variables (battery power P_{bat} and value of the objective function J).

are given by:

$$v_{bat,min} \leq v_{bat} \leq v_{bat,max} \quad (12)$$
$$SOC_{min} \leq SOC \leq SOC_{max} \quad (13)$$
$$i_{bat,min} \leq i_{bat} \leq i_{bat,max} \quad (14)$$
$$P_{grid,min} \leq P_{grid} \leq P^*_{grid} \quad (15)$$
$$P_{PV} \leq P^*_{PV} \quad (16)$$
$$P_{bat} \leq P_{N,conv} \quad (17)$$

3.2. Energy dispatch optimisation using dynamic programming

A dynamic programming (DP) approach is used to maximise the objective function. This technique is based on the principle of optimality, as described by R. Bellman [45]. DP is chosen as the optimisation method because it can deal with nonlinear systems and it does not converge to local optimums. Its main drawback is the relatively large computational time needed to solve complex problems compared to linear algorithms, which limits its applicability in on-line applications. In our case, which is a simulation study, optimisation time is not a constraint.

As shown in Figure 4, the DP algorithm constitutes the core of the energy dispatch optimiser. Moreover, it uses the models described in this paper for the PV system (Subsection 2.2) and the battery system (Subsection 2.3), including their required power converters. The input variables of the DP algorithm are the system and battery characteristics (including its state of health, SOH), the available photovoltaic power calculated from the weather conditions and the electricity price during the time interval studied. In order to run this algorithm, the objective function (Equation 11) needs to be time-discretised. The number of time steps that are addressed by the optimisation problem (N) is an important parameter to define the size of the problem, since this is the number of decision variables $[P_{bat,1} ... P_{bat,N}]$. Taking into account the PV generation daily pattern, the optimisation problem is reduced

to 24 h. Moreover, time steps of one hour ($\Delta t = 1$ h) are chosen, since the electricity price has an hourly pattern in most markets:

$$J = \sum_{k=1}^{24} \left[\left(P_{grid,\mathrm{PV-bat}} - P_{grid,\mathrm{PV}} \right)_k \cdot PC_{elec,k} + \Delta SOH_k \cdot PC_{bat} \right] \quad (18)$$

The states used are the SOC of the battery at each time step (SOC_k), and the relationship between these states is described by the following discretization of Equation 5:

$$SOC_k = SOC_{k-1} - \frac{i_{bat,k}}{C(SOH)} \quad (19)$$

Additionally, the relationship between the current of the battery used in Equation 19 and the battery power is established based on the battery model. Therefore, 24 decision variables need to be calculated by the energy dispatch optimiser (EDO) ($P_{bat,k}$, with k=1...24). The EDO needs to be solved for each of the studied days, making it possible to update the values of the battery capacity and internal resistance, thereby taking the ageing phenomena into account.

3.3. Battery size optimisation using a region-elimination technique

The battery size optimiser is based on the results obtained by the subsequent application of the EDO for each of the days during a whole sample year. These results are used to determine the optimal installed capacity of the ESS that maximises the performance of the overall system. With this approach, the battery sizing and its subsequent management are considered as a whole, which has particular significance given that the sizing of an ESS depends on the management system, which in turn is calculated taking its size into account. Therefore, the overall optimisation of the system can only be achieved by this comprehensive approach. Moreover, the battery sizing is a key part of the PV–battery plant design process, given that the profitability of the battery is affected by its size. On the one hand, if the ESS is too small, it does not allow for the storage and management of the excess PV energy, thereby limiting the revenue achieved. On the other hand, if its capacity is too large, then the investment costs are higher. Therefore, the selection of the optimal battery size involves a trade-off between the battery capacity and price.

A schematic of the battery size optimiser (BSO) is shown in Figure 3. Given that the EDO described in Subsection 3.2 manages the ESS, this algorithm must be run for each BSO iteration step, as shown in the figure. The objective of the ESS designer must be the same as that of the battery management in order to achieve a rational design. Therefore, the EDO and BSO must have the same objective function (Equation 18). The complexity of this optimisation problem is much lower than that of the EDO explained in Subsection 3.2 because the BSO has only one decision variable (the size of the battery), while the EDO has 24. Therefore, considering that the objective function for the BSO is a unimodal function, a region-elimination technique is used for this optimisation. Unimodality means that there is only one maximum in the interval analysed. The region-elimination technique is based on this characteristic of the economic revenue related to battery size. This algorithm evaluates the objective function for different battery sizes and eliminates regions that cannot host the optimal solution, thereby narrowing down the area in which the optimal value for the objective function is reached, as shown in Figure 5. The battery sizes analysed during the subsequent iteration steps belong to the interval defined by the three battery sizes that lead to the three highest revenues to the moment. The strategy used to determine the battery size for each step is divided into two stages. The first three battery sizes to be analysed depend on the PV plant size ($C_1 = 0.5$ kWh/kWp, $C_2 = 2$ kWh/kWp, $C_3 = 5$ kWh/kWp). For the following iterations, the calculated capacities are arranged such that $C_1 < C_2 < ... < C_k$. The capacity (C_m) that provides the maximum value for the objective function is selected, as well as C_{m-1} or alternatively C_{m+1}. The average of these selected capacities is chosen as the value of C_{k+1}, as shown in Figure 5.

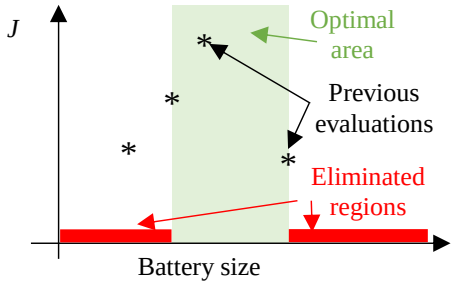

Figure 5: Schematic of the optimisation process carried out by a region-elimination technique. The optimal storage capacity is selected from the optimal area (asterisks in the figure), the objective function is evaluated and this area is narrowed down.

There are several options for detecting the optimal value, which stops the algorithm. Three of the most commonly-used approaches are (*i*) a given number of iterations is reached, (*ii*) the difference between the value of J in two successive iterations is lower than a predefined value, or (*iii*) the optimal area is narrower than a value. Given that simulation time is not a limiting variable for this study, approach (*i*) is chosen and $n = 10$ is selected as the number of iterations, given that sufficient accuracy is achieved in a reasonable optimisation time.

4. Comparison with other optimisers

The proposed global optimisation algorithm is applied in this section to the case study described in Section 2 and compared to two other approaches in order to quantify the improvement in the NPV achieved by our proposal. The performance of each algorithm is described in the following three subsections and their results are summarised in Table 4. Given that the two first algorithms do not take into account the sizing of the battery, the size proposed in a recent research study is chosen [46] (1 kWh per kWp of PV plant). The first algorithm is a commonly-used battery management strategy when the battery cannot be modelled. It lacks of optimisation tool. The second algorithm optimises the management strategy with no consideration about the battery size, which is a typical proposal in the literature. Finally, the third algorithm is the proposal presented in this paper. The performance of the PV–battery plant during the entire lifetime of the battery is simulated in order to achieve this comparison.

4.1. Intuitive algorithm

The intuitive algorithm is based on the battery charging while the available PV power exceeds the maximum grid feed-in limit. Figure 6 (a) and (b) show its performance during a sample day, specifically 2 October 2016. Figure 6 (a) shows the power flows defined in Figure 1, with an hourly time step, as well as the measured global horizontal irradiance (GHI) with a 10 minutes sampling period. It is noteworthy that, even though the GHI is lower than 800 $\mathrm{W\,m^{-2}}$ (80% of the nominal 1,000 $\mathrm{W\,m^{-2}}$), the power generation at noon is as high as 90% of the nominal PV power. This is due to the oversized PV field described in Section 2.There is excess PV power available between 10:00 h and 15:00 h that day, given the feed-in limit at 60 kW. The battery charging lasts until the maximum charge is reached (14:00 h in the figure). Between 13:00 h and 15:00 h there is excess energy available from solar radiation, but it cannot be fed into the grid (because of power limit) or stored in the battery (because it is already fully charged). This intuitive algorithm discharges the battery during the period when the price paid for the electricity reaches its maximum in order to maximise the economic income. In the example shown in Figure 6 this maximum price is achieved between 18:00 h and 19:00 h. However, given the power limitations of the battery, it cannot be fully discharged in one hour and the battery discharging is prolonged until 20:00 h.

The results obtained with this strategy are summarised in the first column of Table 4. Of particular note is the high annual profit of EUR 3,335. However, this intuitive algorithm does not take the ESS degradation into account and, therefore, the battery lifetime is as short as 6.9 years. Despite the high annual profit, the time needed to pay for the cost of the battery (the payback period) is 7.2 years. Therefore, based on the models described above, the investment is not profitable if the ESS is managed by means of this intuitive algorithm, given that the NPV of the investment is EUR –1,090.

4.2. Energy dispatch optimisation

A dynamic programming based energy dispatch optimiser is applied in this subsection for the management of an ESS. Given that this algorithm does not take the battery sizing into account, the proposed size of 1 kWh per kWp of PV plant is assumed [46].

The power dispatch plan and battery SOC calculated by this algorithm are shown in Figure 6 (c) and (d) for comparison with the previously-described intuitive algorithm. Similarly to the intuitive algorithm, the energy dispatch optimiser charges the battery when there is extra PV power available, while some of the available PV energy needs to be discarded. However, the charging process resulting from this algorithm is slower than the previous one, lasting from 10:00 h to 15:00 h on 2 October 2016, which allows for a lower battery charging current, thereby reducing the current-induced ageing mechanisms in the Li-ion battery. Moreover, the surplus energy is discarded during the first three hours of extra PV power (10:00 h–13:00 h), reducing the time at which the battery is kept at maximum SOC, which limits the side reactions resulting in power and capacity fade. Finally, the battery is discharged from 15:00 h to 20:00 h at a variable current rate. Therefore, the revenue obtained by selling this electricity is lower than the one achieved by the intuitive algorithm.

The relevant results compiled in Table 4 show the improvement achieved by this algorithm compared to the simple dispatch. Given that both use the same battery size of 1 kWh per kWp of PV plant, the cost of the battery is the same, as shown in the second column of Table 4. It is particularly noteworthy that, while the annual profit obtained from the electricity is reduced form EUR 3,335 to EUR 2,774, the battery lifetime is almost doubled from 6.9 to 13.7 years. This makes the NPV positive (EUR 13,870), making the ESS a profitable investment by simply managing the same battery with a more elaborated strategy, which implies no extra cost.

4.3. Global optimisation

The global algorithm proposed in this paper is herein applied to the case study. The most important variables during 2 October 2016 are shown in Figure 7 for comparison with Figure 6. The maximisation of the annual revenue

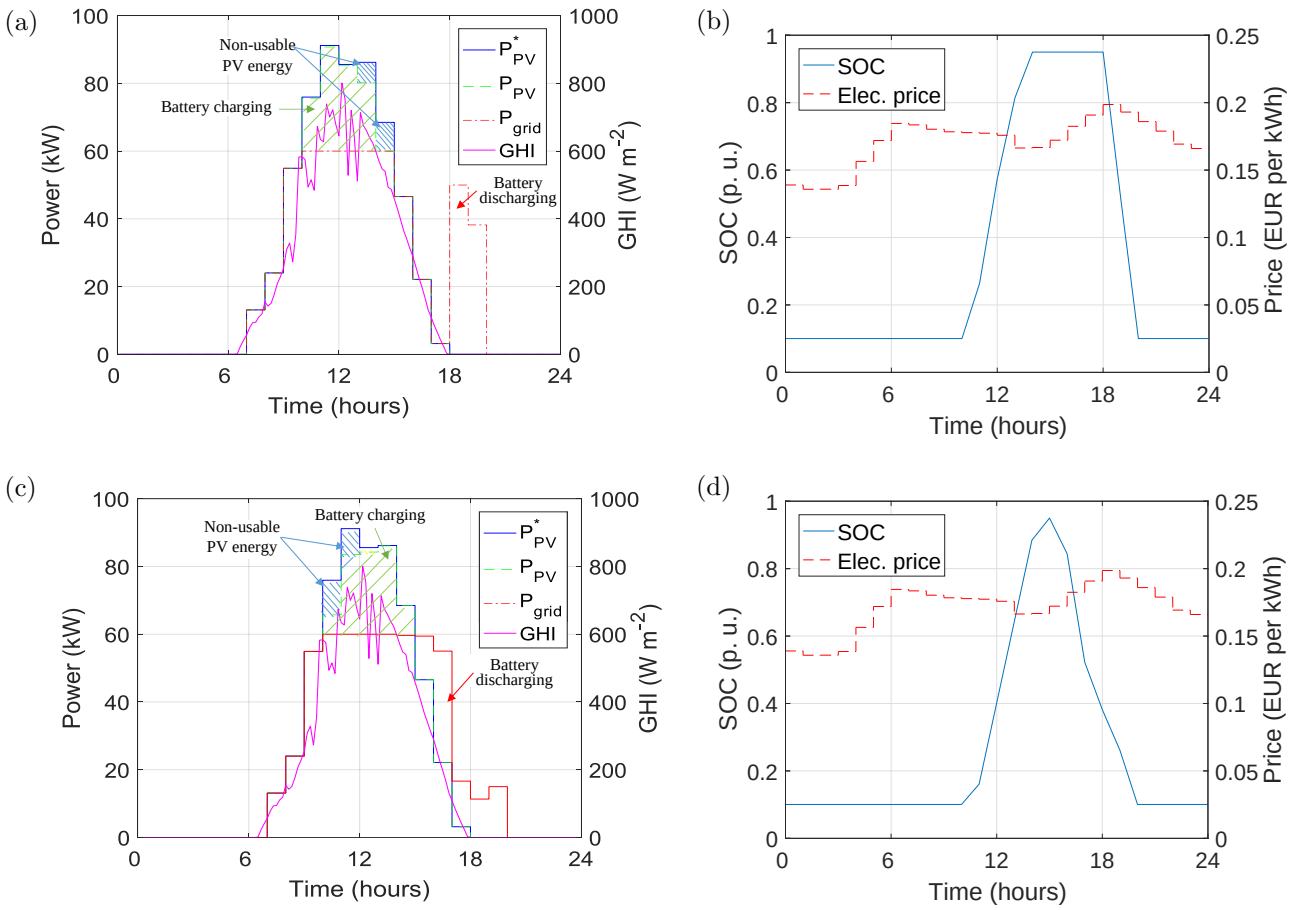

Figure 6: Energy dispatch plan, global horizontal irradiance, battery SOC and electricity price on 2 October 2016 calculated with two algorithms: Intuitive charging and discharging (a) and (b), and proposed EDO (c) and (d).

accounting for the battery sizing and management at the same time gives an optimal battery size of 1.79 kWh per kWp of PV plant, as summarised in the third column of Table 4. This battery size is 79% larger than the 1 kWh per kWp of PV plant used by the previous algorithms.

With regard to the power dispatch calculated by this algorithm, Figure 7 (a) shows that almost all the available PV energy is used either to be fed directly into the grid or to charge the battery. Given the larger size of the battery compared to the one analysed in Figure 6 (c) and (d), there is sufficient capacity to store the surplus energy from 10:00 to 15:00 reaching a maximum SOC of 66%. This reduction in the maximum SOC of the battery leads to slowed ageing phenomena, given that the ageing electrochemical reactions are accelerated by higher voltage. After this charging, the battery discharge is programmed to take place during the afternoon (from 15:00 to 20:00). This slow discharging process results in a lower battery current and, therefore, reduced battery ageing.

The figures of merit for the PV–battery plant optimally managed with the proposed global algorithm are shown in the column *Global* of Table 4. The result of the greater battery size is that the investment (battery price) is 80% larger than that required for the other two algorithms, which allows a less intensive use of the battery, extending its lifetime from 13.7 achieved by the EDO algorithm to 16.42 years. Furthermore, given the greater battery capacity available, less PV energy needs to be discarded, thereby increasing the annual profit of the system. The total revenue of the PV–battery plant, when sized and managed with the proposed global optimiser, increases from EUR 13,870 to EUR 20,178 per year, corresponding to a 22% increase in the NPV.

Table 4: Main magnitudes for the three sizing and management strategies compared.

Strategy	Intuitive	EDO	Global
Battery size (kWh kWp^{-1})	1	1	1.79
Battery price (EUR)	25 000	25 000	44 625
Average annual profit (EUR)	3335	2774	3822
Payback (years)	7.2	8.7	11.14
Battery lifetime (years)	6.9	13.7	16.42
Total revenue (EUR)	−1000	13 870	20 178
NPV (EUR)	−1090	10 448	13 400

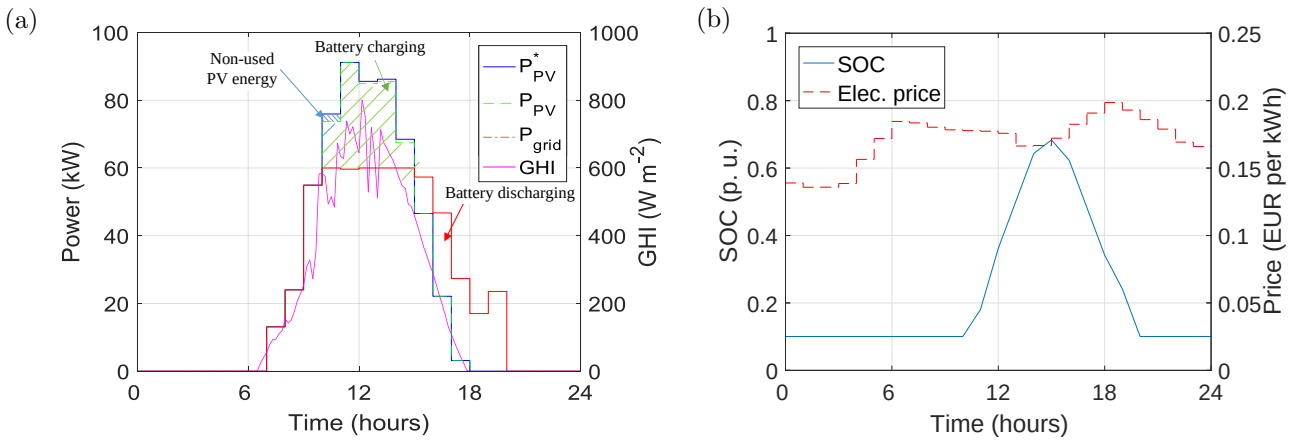

Figure 7: Energy dispatch plan and global horizontal irradiance (a), battery SOC and electricity price (b) on 2 October 2016 calculated with the EDO algorithm for a PV–battery system with a battery sized by means of the BSO algorithm.

Therefore, Table 4 clearly summarises the improvements that the proposed global optimisation algorithm achieves in a PV–battery system compared to other management algorithms. The longer lifetime, added to the higher annual revenue, leads to an increased NPV of the investment, which is the objective function of the optimiser.

5. Sensitivity analysis

As an application of the battery optimisation method proposed in this paper, a sensitivity analysis is presented in this section. This analysis provides information about the most critical variables that influence the NPV of a PV–battery plant. Three magnitudes are chosen as input variables for the sensitivity analysis: (*i*) average electricity price, (*ii*) electricity price range, and (*iii*) ESS cost. The variation interval around their rated values is set to ±20% with a total of seven points (0.8, 0.9, 0.95, 1, 1.05, 1.1 and 1.2 times the nominal value). Finally, the NPV of the PV storage system will be analysed as the output variable. The sensitivity analysis helps to answer questions such as: Is a 10% reduction in battery price more or less profitable than a 10% increase in electricity prices for a PV–battery plant? Which variable is more sensitive for the design of the storage system: average electricity price during the year or the difference between maximum and minimum daily price?

The chosen sensitivity method is the variation of one factor at a time, consisting in setting a standard scenario (the one described in Section 2), defining the studied variables and changing the value of one input variable, while the others are maintained at their nominal values. The variable is then returned its rated value and the process is repeated for the next input variable. Sensitivity is then measured by monitoring changes in the output, as any observed change will unambiguously be due to the single variable changed.

The results of a sensitivity analysis are usually displayed in graphs with the input parameter represented on the horizontal axis and the output variable on the vertical axis. For the sake of comparability, both values are usually normalised, being (1, 1) the central point of each plot. In addition to this plot, a numerical value of the average sensitivity is also useful for easy and accurate comparison of different analyses.

The results of the sensitivity analysis for the PV–battery plant are shown in Figure 8. The circles are the NPV of the PV–battery plant. A straight line is fitted to these markers, whose slope is the average NPV sensitivity to each parameter. The nominal value (1, 1) in the three figures corresponds to an NPV of EUR 13,400, as already reported in Table 4, in which the standard scenario is analysed. The absolute value for each input variable at this point is defined in Section 2, corresponding to an average electricity price of EUR 0.14 per kWh, electricity price range of EUR 0.23 per kWh and a battery price of EUR 250 per kWh.

A variation in the average electricity price is studied in Figure 8 (a). As is to be expected, an increase in this input variable results in a greater NPV of the investment. Moreover, the variation in the NPV is greater than the one for the average electricity price. In fact, a 20% increase in the electricity price leads to an NPV that is more than 2 times higher, which means a sensitivity of 5.31, as reported in Table 5. Therefore, the average electricity price needs to be closely studied during the design and management of such a PV–battery plant, since the variation in the NPV of the investment is five times greater than the original change in electricity price. Figure 8 (b) shows the NPV

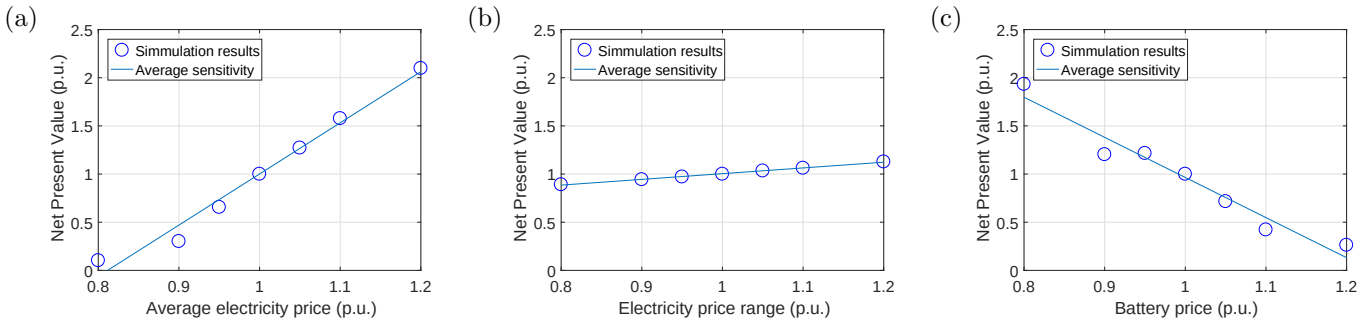

Figure 8: Sensitivity analysis of the NPV to three input variables: average electricity price (a), electricity price range (b), and battery price (c).

Table 5: Average sensitivity of the NPV to three characteristic parameters in a ±20% interval.

Input parameter	Sensitivity of NPV
Average electricity price	5.31
Electricity price range	0.59
Battery price	–4.16

sensitivity to the electricity price range. The points are much closer to 1 and, therefore, the line slope is lower than for the previous case. Indeed, a variation of 20% in the electricity price range only brings a change of 12% in the NPV, representing a sensitivity of 0.59. Finally, Figure 8 (c) shows the sensitivity of NPV to battery price. As expected, it has a downward trend, since as the battery price increases, the investment opportunity decreases. The slope of the line is –4.16. Note that that a 20% increase in ESS costs (and thus an increase in investment) still results in a profitable investment, i.e. NPV>0.

6. Conclusion

A new approach to the sizing and management of Li-ion batteries for the grid integration of renewable energy plants has been described in this paper. This approach is based on a combined dynamic program algorithm and region-elimination technique to achieve the global optimisation of two key problems: the battery sizing and its subsequent management. This comprehensive optimisation makes it possible to both consider the battery size in the design of the management strategy, and calculate its optimal size based on the strategy that will manage the battery during its operation. As a result, the battery lifetime is extended, thereby increasing the profitability of the required investment. After the detailed presentation of the optimisation algorithm, this was then applied to a rooftop PV plant installed in an industrial area, which is an interesting scenario to be studied, given the problems that can arise in industrial estate distribution networks due to the expected increase in these installations in the upcoming years. Finally, a sensitivity analysis identifies interesting variables to be analysed by different decision makers.

The main features offered by the proposed algorithm based on the combined dynamic programming and region-elimination technique are (*i*) its overall approach to the correlated problems of sizing an ESS and its subsequent management, (*ii*) its ability to handle non-linear system models and operational constraints, (*iii*) its ease of adaptation to handle different problems with customised models and constraints, (*iv*) its reduced computational demands, being suitable for a normal laptop, and (*v*) its improved performance, compared to other studies which focus their attention on the management of an arbitrarily-sized battery. This last capability deserves special attention, and a section of the paper offers further details on this issue. With this aim, an objective function is optimised assuming a battery size of 1 Wh per Wp of PV power, as proposed in the literature, and then using the proposed comprehensive algorithm. The comprehensive algorithm achieves a 22% improvement in the objective function, hitting the global optimum of the system.Finally, the influence of three input variables on the NPV of the investment are studied by means of a sensitivity analysis.

Two new research lines arise as a consequence of this paper. On the one hand, an accelerated algorithm would allow for the on-line optimisation of the battery management by means of a typical microcontroller. On the other hand, the capability of the algorithm to manage shorter time steps (with the subsequent increase of optimisation variables) would allow the study of faster battery charge–discharge cycles and its implications related to battery ageing.

Due to the good performance of the algorithm shown in the case study, as well as its flexibility and ease of use, it can be considered to be a useful tool for the sizing and management of energy storage systems connected to renewable power plants.

Acknowledgements

We would like to acknowledge the support of the Spanish State Research Agency and FEDER–UE under grants DPI2016–80641–R and DPI2016–80642–R; of Government of Navarra through research project PI038 INTEGRA-RENOVABLES; and the FPU Program of the Spanish Ministry of Education, Culture and Sport (FPU13/00542).

References

References

[1] A. Zervos, Renewables 2016 global status report, Technical report, REN21 Renewable Energy Policy Network for the 21st Century (2016).

[2] A. Steiner, C. Köhler, I. Metzinger, A. Braun, M. Zirkelbach, D. Ernst, P. Tran, B. Ritter, Critical weather situations for renewable energies - Part A: Cyclone detection for wind power, Renewable Energy 101 (2017) 41 – 50 (2017). doi:http://dx.doi.org/10.1016/j.renene.2016.08.013.

[3] C. Köhler, A. Steiner, Y.-M. Saint-Drenan, D. Ernst, A. Bergmann-Dick, M. Zirkelbach, Z. Ben Bouallègue, I. Metzinger, B. Ritter, Critical weather situations for renewable energies - Part B: Low stratus risk for solar power, Renewable Energy 101 (2017) 794–803 (2017). doi:10.1016/j.renene.2016.09.002.

[4] M. Steuer, U. Fahl, A. Voß, Curtailment: an option for cost-efficient integration of variable renewable generation, Tech. rep., The INSIGHT_E project (10 2014).

[5] A. Nottrott, J. Kleissl, B. Washom, Energy dispatch schedule optimization and cost benefit analysis for grid-connected, photovoltaic-battery storage systems, Renewable Energy 55 (2013) 230–240, cited By 46 (2013). doi:10.1016/j.renene.2012.12.036.

[6] Tesla, Tesla powerwall, online.
URL https://www.tesla.com/powerwall?redirect=no

[7] P. Cazzola, M. Gorner, Global EV outlook 2016, Technical report, International Energy Agency (2016).

[8] C. Xie, Y. Hong, Y. Ding, Y. Li, J. Radcliffe, An economic feasibility assessment of decoupled energy storage in the UK: With liquid air energy storage as a case study, Applied Energy 225 (2018) 244 – 257 (2018). doi:https://doi.org/10.1016/j.apenergy.2018.04.074.

[9] C. S. Lai, M. D. McCulloch, Levelized cost of electricity for solar photovoltaic and electrical energy storage, Applied Energy 190 (2017) 191 – 203 (2017). doi:https://doi.org/10.1016/j.apenergy.2016.12.153.

[10] G. Mulder, D. Six, B. Claessens, T. Broes, N. Omar, J. V. Mierlo, The dimensioning of PV–battery systems depending on the incentive and selling price conditions, Applied Energy 111 (2013) 1126 – 1135 (2013). doi:http://dx.doi.org/10.1016/j.apenergy.2013.03.059.

[11] D. Parra, M. K. Patel, Effect of tariffs on the performance and economic benefits of PV-coupled battery systems, Applied Energy 164 (2016) 175 – 187 (2016). doi:https://doi.org/10.1016/j.apenergy.2015.11.037.

[12] K. Uddin, R. Gough, J. Radcliffe, J. Marco, P. Jennings, Techno-economic analysis of the viability of residential photovoltaic systems using lithium-ion batteries for energy storage in the United Kingdom, Applied Energy 206 (2017) 12 – 21 (2017). doi:https://doi.org/10.1016/j.apenergy.2017.08.170.

[13] A. Mariaud, S. Acha, N. Ekins-Daukes, N. Shah, C. N. Markides, Integrated optimisation of photovoltaic and battery storage systems for UK commercial buildings, Applied Energy 199 (2017) 466 – 478 (2017). doi:https://doi.org/10.1016/j.apenergy.2017.04.067.

[14] L. I. Minchala Avila, L. E. Garza-Castañón, A. Vargas-Martínez, Y. Zhang, A review of optimal control techniques applied to the energy management and control of microgrids, Procedia Computer Science 52 (2015) 780 – 787 (2015). doi:http://dx.doi.org/10.1016/j.procs.2015.05.133.

[15] H. Zhao, Q. Wu, S. Hu, H. Xu, C. N. Rasmussen, Review of energy storage system for wind power integration support, Applied Energy 137 (2015) 545 – 553 (2015). doi:http://dx.doi.org/10.1016/j.apenergy.2014.04.103.

[16] E. Waffenschmidt, Dimensioning of decentralized photovoltaic storages with limited feed-in power and their impact on the distribution grid, Energy Procedia 46 (2014) 88 – 97, 8th International Renewable Energy Storage Conference and Exhibition (IRES 2013) (2014). doi:http://dx.doi.org/10.1016/j.egypro.2014.01.161.

[17] O. Mégel, J. L. Mathieu, G. Andersson, Scheduling distributed energy storage units to provide multiple services under forecast error, International Journal of Electrical Power & Energy Systems 72 (2015) 48 – 57, the Special Issue for 18th Power Systems Computation Conference. (2015). doi:http://dx.doi.org/10.1016/j.ijepes.2015.02.010.

[18] G. de Oliveira e Silva, P. Hendrick, Photovoltaic self-sufficiency of Belgian households using lithium-ion batteries, and its impact on the grid, Applied Energy 195 (2017) 786 – 799 (2017). doi:https://doi.org/10.1016/j.apenergy.2017.03.112.

[19] S. Quoilin, K. Kavvadias, A. Mercier, I. Pappone, A. Zucker, Quantifying self-consumption linked to solar home battery systems: Statistical analysis and economic assessment, Applied Energy 182 (2016) 58 – 67 (2016). doi:https://doi.org/10.1016/j.apenergy.2016.08.077.

[20] J. M. Reniers, G. Mulder, S. Ober-Blöbaum, D. A. Howey, Improving optimal control of grid-connected lithium-ion batteries through more accurate battery and degradation modelling, Journal of Power Sources 379 (2018) 91 – 102 (2018). doi:https://doi.org/10.1016/j.jpowsour.2018.01.004.

[21] J. Li, M. A. Danzer, Optimal charge control strategies for stationary photovoltaic battery systems, Journal of Power Sources 258 (2014) 365 – 373 (2014). doi:http://dx.doi.org/10.1016/j.jpowsour.2014.02.066.

[22] J. Weniger, J. Bergner, V. Quaschning, Integration of PV power and load forecasts into the operation of residential PV battery systems, in: 4th Solar Integration Workshop, 2014 (2014).

[23] M. Nemati, M. Braun, S. Tenbohlen, Optimization of unit commitment and economic dispatch in microgrids based on genetic algorithm and mixed integer linear programming, Applied Energy 210 (2018) 944 – 963 (2018). doi:https://doi.org/10.1016/j.apenergy.2017.07.007.

[24] R. Xiong, Y. Duan, J. Cao, Q. Yu, Battery and ultracapacitor in-the-loop approach to validate a real-time power management method for an all-climate electric vehicle, Applied Energy 217 (2018) 153 – 165 (2018). doi:https://doi.org/10.1016/j.apenergy.2018.02.128.

[25] B. D. Olaszi, J. Ladanyi, Comparison of different discharge strategies of grid-connected residential PV systems with energy storage in perspective of optimal battery energy storage system sizing, Renewable and Sustainable Energy Reviews 75 (2017) 710 – 718 (2017). doi:http://dx.doi.org/10.1016/j.rser.2016.11.046.

[26] S. Barsali, R. Giglioli, G. Lutzemberger, D. Poli, G. Valenti, Optimised operation of storage systems integrated with MV photovoltaic plants, considering the impact on the battery lifetime, Journal of Energy Storage 12 (2017) 178 – 185 (2017). doi:http://dx.doi.org/10.1016/j.est.2017.05.003.

[27] H. Wang, M. Muñoz-García, G. Moreda, M. Alonso-García, Optimum inverter sizing of grid-connected photovoltaic systems based on energetic and economic considerations, Renewable Energy 118 (2018) 709 – 717 (2018). doi:https://doi.org/10.1016/j.renene.2017.11.063.

[28] AEMET, Gobierno de Navarra, Meteorología y climatología de Navarra, online.
URL http://meteo.navarra.es/estaciones/mapadeestaciones.cfm

[29] R. Dufo López, J. L. Bernal-Agustín, Techno-economic analysis of grid-connected battery storage, Energy Conversion and Management 91 (2015) 394 – 404 (2015). doi:http://dx.doi.org/10.1016/j.enconman.2014.12.038.

[30] S. N. Laboratories, Pvperformance: Modeling collaborative, online.
URL https://pvpmc.sandia.gov/applications/pv_lib-toolbox/

[31] A. Driesse, P. Jain, S. Harrison, Beyond the curves: Modeling the electrical efficiency of photovoltaic inverters, in: 2008 33rd IEEE Photovoltaic Specialists Conference, 2008, pp. 1–6 (May 2008). doi:10.1109/PVSC.2008.4922827.

[32] M. Jantsch, Systemtechnische Untersuchung des Nutzungsgrades photovoltaischer Anlagen: Analyse und Optimierung von Strukturen und Wirkungszusammenhängen, Fortschritt-Berichte VDI. Reihe 6, Energietechnik, VDI-Verlag, 1996 (1996).

[33] A. Berrueta, V. Irigaray, P. Sanchis, A. Ursúa, Lithium-ion battery model and experimental validation, in: Power Electronics and Applications (EPE'15 ECCE-Europe), 2015 17th European Conference on, 2015, pp. 1–8 (Sept 2015). doi:10.1109/EPE.2015.7309337.

[34] A. Berrueta, I. S. Martín, P. Sanchis, A. Ursúa, Comparison of state-of-charge estimation methods for stationary lithium-ion batteries, in: IECON 2016 - 42nd Annual Conference of the IEEE Industrial Electronics Society, 2016, pp. 2010–2015 (Oct 2016). doi:10.1109/IECON.2016.7794094.

[35] A. Berrueta, A. Urtasun, A. Ursúa, P. Sanchis, A comprehensive model for lithium-ion batteries: From the physical principles to an electrical model, Energy 144 (2018) 286–300 (2018). doi:10.1016/j.energy.2017.11.154.

[36] W. Waag, C. Fleischer, D. U. Sauer, Critical review of the methods for monitoring of lithium-ion batteries in electric and hybrid vehicles, Journal of Power Sources 258 (2014) 321 – 339 (2014). doi:http://dx.doi.org/10.1016/j.jpowsour.2014.02.064.

[37] C. Weng, X. Feng, J. Sun, H. Peng, State-of-health monitoring of lithium-ion battery modules and packs via incremental capacity peak tracking, Applied Energy 180 (2016) 360 – 368 (2016). doi:https://doi.org/10.1016/j.apenergy.2016.07.126.

[38] C. Campestrini, P. Keil, S. F. Schuster, A. Jossen, Ageing of lithium-ion battery modules with dissipative balancing compared with single-cell ageing, Journal of Energy Storage 6 (2016) 142 – 152 (2016). doi:https://doi.org/10.1016/j.est.2016.03.004.

[39] J. Schmalstieg, S. Käbitz, M. Ecker, D. U. Sauer, A holistic aging model for li(nimnco)o_2 based 18650 lithium-ion batteries, Journal of Power Sources 257 (2014) 325 – 334 (2014). doi:http://dx.doi.org/10.1016/j.jpowsour.2014.02.012.

[40] J. Schmitt, A. Maheshwari, M. Heck, S. Lux, M. Vetter, Impedance change and capacity fade of lithium nickel manganese cobalt oxide-based batteries during calendar aging, Journal of Power Sources 353 (2017) 183 – 194 (2017). doi:http://dx.doi.org/10.1016/j.jpowsour.2017.03.090.

[41] J. Wang, J. Purewal, P. Liu, J. Hicks-Garner, S. Soukazian, E. Sherman, A. Sorenson, L. Vu, H. Tataria, M. W. Verbrugge, Degradation of lithium ion batteries employing graphite negatives and nickel–cobalt–manganese oxide + spinel manganese oxide positives: Part 1, aging mechanisms and life estimation, Journal of Power Sources 269 (2014) 937 – 948 (2014). doi:http://dx.doi.org/10.1016/j.jpowsour.2014.07.030.

[42] J. Purewal, J. Wang, J. Graetz, S. Soukiazian, H. Tataria, M. W. Verbrugge, Degradation of lithium ion batteries employing graphite negatives and nickel–cobalt–manganese oxide + spinel manganese oxide positives: Part 2, chemical–mechanical degradation model, Journal of Power Sources 272 (2014) 1154 – 1161 (2014). doi:http://dx.doi.org/10.1016/j.jpowsour.2014.07.028.

[43] J. Schmalstieg, S. Käbitz, M. Ecker, D. U. Sauer, From accelerated aging tests to a lifetime prediction model: Analyzing lithium-ion batteries, in: 2013 World Electric Vehicle Symposium and Exhibition (EVS27), 2013, pp. 1–12 (Nov 2013). doi:10.1109/EVS.2013.6914753.

[44] S. F. Schuster, T. Bach, E. Fleder, J. Müller, M. Brand, G. Sextl, A. Jossen, Nonlinear aging characteristics of lithium-ion cells under different operational conditions, Journal of Energy Storage 1 (2015) 44 – 53 (2015). doi:http://dx.doi.org/10.1016/j.est.2015.05.003.

[45] R. Bellman, Dynamic Programming, 1st Edition, Princeton University Press, Princeton, NJ, USA, 1957 (1957).

[46] S. T. Kim, S. Bae, Y. C. Kang, J. W. Park, Energy management based on the photovoltaic HPCS with an energy storage device, IEEE Transactions on Industrial Electronics 62 (7) (2015) 4608–4617 (July 2015). doi:10.1109/TIE.2014.2370941.